

# Quantum and classical Josephson oscillations for a Bose-Einstein condensate

Juha Javanainen<sup>1</sup> and Janne Ruostekoski<sup>2</sup>

<sup>1</sup>*Department of Physics, University of Connecticut, Storrs, Connecticut 06269-3046*

<sup>2</sup>*School of Mathematics, University of Southampton, Southampton, SO17 1BJ, UK*

We study a Bose-Einstein condensate in a double-well trap when the atom number in each potential well is monitored continuously via light scattering. The quantum mechanical solution and an ab-initio classical stochastic description that incorporates the back-action of the atom number measurements as phase diffusion are compared for the Josephson oscillations. The conjecture emerges that if the continuous measurements can resolve the classical behavior, that is what they will report.

PACS numbers: 03.75.Lm, 03.65.Ta, 05.30.Jp

Experimental techniques with the double-well trap containing a Bose-Einstein condensate [BEC] [1–3] and with the internal Josephson effect [4] are now at the point when the details of the nonlinear mean-field dynamics [5] of the condensate can be probed. Going on to smaller atom numbers will inevitable bring up the issue of quantum versus classical dynamics. Basically in the limit of a large atom number, we have demonstrated how the back-action of continuous measurements of the atom numbers on both sides of the trap induces quantum mechanics to mimic unstable classical dynamics [6]. A related discussion of the dynamical manifestations of chaos in quantum mechanics has continued for a while [7–10].

Here we work our way toward smaller atom numbers: How accurately can classical physics describe the double-well system when quantum mechanics seems to be the natural language? A system that is never observed cannot serve any useful function, and according to quantum mechanics every observation incurs a measurement back-action. The back-action therefore takes on a prominent role: even if we insist on a *classical* description [11] of a sufficiently small system, it has to be incorporated. Our immediate goal is to demonstrate how to do this.

We analyze a double-well trap containing a BEC, assuming that the atom numbers on both sides are monitored continuously using light scattering as the atoms oscillate back and forth between the traps. We set up the exact quantum mechanical time evolution, and also develop a classical approach, an elaboration upon both mean-field theory [5] and the usual Truncated Wigner Approximation (TWA) [12–15], in which the measurement back-action is included as diffusion of the phase difference of the BECs in the two halves of the trap. We find, again [6], that if the measurements can resolve the classical time evolution, that is what they will report. The second objective of this Letter is to promote this observation as an organizing principle.

We employ the two-mode approximation [16, 17], the two-site version of the Bose-Hubbard model. Denoting the boson operators for the atoms in the two potential wells by  $a$  and  $b$ , we have the Hamiltonian with a hopping amplitude  $J$ , strength of atom-atom interaction  $U$ , and an imbalance in the energies of the atoms between the

sides  $\epsilon$ ,

$$H = -J(a^\dagger b + b^\dagger a) + U(a^\dagger a^\dagger a a + b^\dagger b^\dagger b b) + \epsilon(a^\dagger a - b^\dagger b). \quad (1)$$

For the sake of transparency we set  $\hbar = 1$ .

We assume that the atom numbers in each well are measured by light scattering, ultimately using detectors that count photons one by one. This adds a Lindblad type relaxation term [18] to the equation of motion of the density operator  $\rho$  for the double-well system

$$\mathcal{L}\rho = \sum_{i=a,b} \left[ L_i \rho L_i^\dagger - \frac{1}{2}(\rho L_i^\dagger L_i + L_i^\dagger L_i \rho) \right]. \quad (2)$$

We have  $L_a = \sqrt{\Gamma} a^\dagger a$  and  $L_b = \sqrt{\Gamma} b^\dagger b$ .  $\Gamma$  specifies the strength of the measurements and can be adjusted, for instance, by varying the intensity or the frequency of the probing light. All told, we have the master equation

$$\dot{\rho} = -i[H, \rho] + \mathcal{L}\rho. \quad (3)$$

Here the rates of photon detection are proportional to the squares of the atom numbers in the respective potential wells [19]. Such a model for atom detection can be realized by off-resonant light scattering; in principle, the more accurately the larger is the total number of atoms and the smaller in size are the BECs [20].

To develop the parallel classical description we begin by rewriting the master equation in terms of the Wigner function  $W(\alpha, \alpha^*, \beta, \beta^*; t)$ , where  $\alpha$  and  $\beta$  are complex numbers corresponding to the operators  $a$  and  $b$  [18, 21]. In the equation of motion of the Wigner function,  $\alpha$ ,  $\alpha^*$  and  $\beta$ ,  $\beta^*$  will behave like canonical pairs with Poisson brackets such as  $\{\alpha, \alpha^*\} = -i$ . In the next step we move on to four real variables  $N$ ,  $\Phi$ ,  $Z$  and  $\varphi$  defined by

$$\alpha = \sqrt{\frac{1}{2}N - Z} e^{i(\Phi - \frac{1}{2}\varphi)}, \quad \beta = \sqrt{\frac{1}{2}N + Z} e^{i(\Phi + \frac{1}{2}\varphi)}. \quad (4)$$

The transformation from the original variables is canonical, and results in Poisson brackets such as  $\{Z, \varphi\} = 1$ .

While there is a straightforward relation between the quantities  $a$  and  $\alpha$  and likewise for  $b$  and  $\beta$ , there probably are no hermitian quantum operators corresponding to the newly defined angle variables  $\Phi$  and  $\varphi$ . Instead, to the extent possible, we regard the Wigner function as the classical joint probability density for total atom number

$N$ , imbalance of atom numbers on each side of the double well  $Z$ , overall phase of the two BECs  $\Phi$ , and phase difference of the BECs between the two potential wells  $\varphi$ .

The global phase  $\Phi$  has no dynamics, nor any relevance to the dynamics of the other variables. Furthermore, we scale to the limit of a large total number of the atoms  $N$  in the following way. First, the classical mean-field theory for the BEC amplitudes tends to become increasingly accurate when the atom-atom interaction  $U$  is scaled down with an increasing number of atoms so that  $NU = \chi$  remains a constant. Thus we write  $U = \chi/N$ . Likewise, we define a new variable  $z = 2Z/N$ , which is the fractional difference in the atom numbers between the sides;  $z \in [-1, 1]$ . To the leading order in the total atom number  $N$  the equation of motion of the remaining distribution function  $W(z, \varphi; t)$  is

$$\partial_t W = \left[ -\frac{\partial h}{\partial \varphi} \partial_z + \frac{\partial h}{\partial z} \partial_\varphi + \Gamma \partial_{\varphi\varphi} \right] W, \quad (5)$$

with

$$h(z, \varphi) = z^2 \chi - 2\epsilon z - 2J\sqrt{1-z^2} \cos(\varphi). \quad (6)$$

We have dropped third-order derivatives, which are formally of the order  $N^{-2}$ .

The first-order derivatives in Eq. (5) constitute the Liouville equation of the distribution function for the variables  $z$  and  $\varphi$  under the Hamiltonian  $h$ . As such, they describe the probability distribution of  $z$  and  $\varphi$  in an ensemble of BECs, each of which evolves according to the mean field theory [5]. Most remarkably, though, the quantum mechanical back-action of the measurements of the particle numbers has added a diffusion  $\propto \Gamma \partial_{\varphi\varphi}$  to the relative phase of the BECs. This contribution is classical; if  $W$  is a valid classical probability distribution function at some time, it remains so during all subsequent evolution under Eq. (5).

We discuss quantum and classical evolutions in the case when the system is first prepared to a zero-temperature thermal equilibrium in the presence of an energy imbalance  $\epsilon \neq 0$ , and the imbalance is then suddenly removed. The result is oscillations of the atoms between the two sides of the potential well.

In the quantum analysis the evolution of the density operator according to Eq. (3) is solved using quantum trajectory simulations [22–24]. Basically, for every run of the simulations we have a state vector that undergoes “quantum jumps” at random times. A collection of  $N_S$  stochastically generated time dependent state vectors is used to describe the state of the system. Given an observable  $A$ , the expectation value for these state vectors averaged over the  $N_S$  realizations approximates the quantum expectation value  $\text{Tr}[\rho(t)A]$ . We denote such an expectation value by  $\langle\langle A(t) \rangle\rangle_Q$ . For instance, the quantum counterpart of the population imbalance  $\hat{z} = (2b^\dagger b - N)/N$  from the simulations is  $z_Q(t) = \langle\langle \hat{z}(t) \rangle\rangle_Q$ . Fluctuations of the population imbalance are also of interest in quantitative comparisons between quantum mechanics and classical physics, but here our focus is on qualitative features.

The setup of the classical analysis requires more care. First, corresponding to the quantum fluctuations in the initial state, we introduce fluctuation also in the classical state. Suppose Eq. (5) were written in terms of the variables  $Z$  and  $\varphi$  instead of  $z$  and  $\varphi$ , and likewise for the Hamiltonian  $\mathcal{H}$  generating the time evolution. We expand Hamiltonian  $\mathcal{H}(Z, \varphi)$  to second order in  $Z$  and  $\varphi$  around the classical lowest-energy state as prepared in the presence of the initial imbalance  $\epsilon \neq 0$  between the sides. Now, since the classical variables  $Z$  and  $\varphi$  are a canonical pair, we may *requantize* by postulating the commutator  $[Z, \varphi] = i$ .  $\mathcal{H}(Z, \varphi)$  thereby becomes the quantum Hamiltonian of a harmonic oscillator. The Wigner function corresponding to the ground state of this oscillator is used as the initial distribution of the variables  $Z$  and  $\varphi$ , and immediately gives the initial distribution of the variables  $z$  and  $\varphi$ . We take  $\chi > 0$  and choose  $\epsilon$  in such a way that the classical equilibrium has the phase  $\varphi = 0$  and a predetermined population imbalance  $z = f$ . The initial Wigner function is then approximated by

$$W(z, \varphi) = \frac{N}{2\pi} \exp \left[ -\frac{N}{2} \left( \frac{(z-f)^2}{\beta} + \beta \varphi^2 \right) \right], \quad (7)$$

$$\beta = \frac{1-f^2}{\sqrt{1+(1-f^2)^{3/2}\chi/J}}. \quad (8)$$

We are now in a position to state precisely what “classical description” [11] entails in this context: the Wigner function remains a valid probability density at all times under consideration. The standard mean field theory [5] and TWA [12–15] are classical descriptions, and so is also the combination of Eqs. (5) and (7). This particular classical description has its origin in quantum mechanics and approximately includes measurement back-action, but at this point it is entirely conventional stochastic analysis.

If there were no phase diffusion in the time evolution (5), by repeatedly sampling initial states  $(z, \varphi)$  from the distribution (7) and letting them evolve under the Hamiltonian  $h$ , this time with  $\epsilon = 0$ , we would have a collection of trajectories  $(z(t), \varphi(t))$  that makes the usual TWA [12–15] of the original quantum problem. However, an additional phase diffusion is present. Correspondingly, we add a suitable Langevin noise term to the evolution [25]. Over the time  $dt$   $z$  and  $\varphi$  therefore change by

$$dz = 2J\sqrt{1-z^2} \sin \varphi dt, \quad (9)$$

$$d\varphi = -2z \left( \chi + J \frac{\cos \varphi}{\sqrt{1-z^2}} \right) dt + \sqrt{2\Gamma} dW(t), \quad (10)$$

where  $dW(t)$  is a random increment of the Wiener process over the interval  $dt$ . The stochastic dynamical equations are integrated using the Milstein algorithm [25]. Given a collection of classical trajectories, the expectation value of a quantity  $A$ ,  $\langle\langle A(t) \rangle\rangle_C$ , is obtained by averaging the values of  $A$  over the  $N_S$  trajectories at time  $t$ . In this way we have the classical expectation value  $z_C(t)$  of the population imbalance.

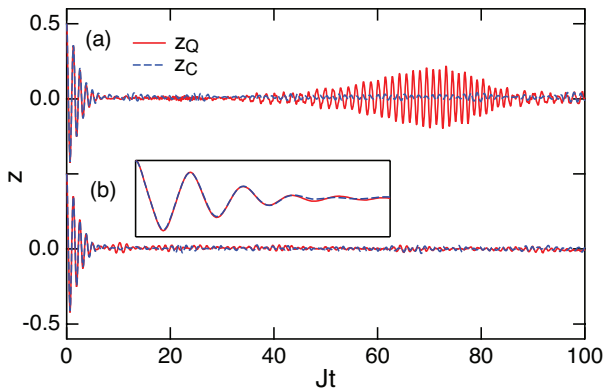


FIG. 1. (Color online) Quantum (solid lines) and classical (dashed lines) expectation values of population imbalance  $z$  as a function of time  $t$ . Graph (a) is without continuous monitoring,  $\Gamma/J = 0$ , graph (b) corresponds to the observation strength  $\Gamma/J = 0.003$ . The atom number is  $N = 100$ , the atom-atom interaction strength is  $\chi/J = 10$ , the initial population imbalance is  $f = 0.5$ , and the number of both classical and quantum simulations averaged in these graphs is  $N_S = 1,000$ . The inset demonstrates the quality of the quantum-classical agreement in the collapse part of trace (b).

As the first example of the results consider Fig. 1. The atom number is fixed precisely at  $N = 100$ , the rest of the parameters are  $\chi/J = 10$ ,  $f = 0.5$ , and  $N_S = 1,000$ . Panel (a) with no measurements at all,  $\Gamma = 0$ , plots the quantum (solid line) and classical (dashed line) expectation values of the population imbalance. The quantum and classical values both show a collapse up to  $Jt \simeq 10$ , but only the quantum expectation value has a revival at around  $Jt = 70$ .

In Fig. 1(b) we turn on the measurements with  $\Gamma/J = 0.003$ . This value is chosen so that on the average the right detector reports about ten photons during one back-and-forth swing of the atoms between the traps. The oscillations of the atoms should therefore be easily resolved by light scattering. The collapse part, quantum and classical, is almost unchanged by the measurements, but the quantum revival has disappeared as a result of the measurement back-action. With the measurements on, the quantum and classical analyses agree very well.

A quantum trajectory simulation with its quantum jumps produces a faithful simulation of one individual experimental realization, each quantum jump corresponding to a detection of a photon [18]. From the known times of the quantum jumps one may deduce an approximation for the instantaneous population imbalance  $z(t)$  in various ways on the basis of the observation that the instantaneous counting rate is proportional to the square of the number of the atoms. Here, however, we proceed differently. Given a quantum trajectory, we use the expectations value of  $\hat{z}$  in this single trajectory (quantum state)  $z_Q(t)$  to approximate the value of the population imbalance that one would deduce from the quantum jumps. We are attempting to reconcile observations of discrete photon counts with a picture that the atoms oscillate be-

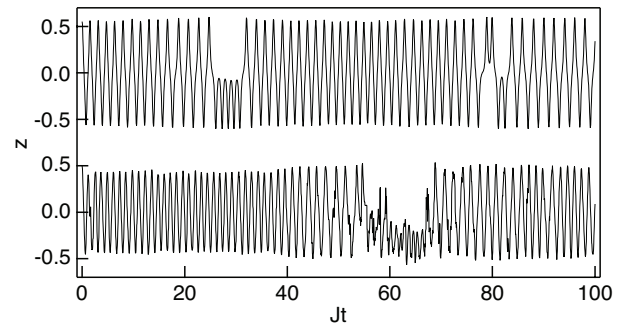


FIG. 2. An individual classical (upper trace) and quantum (lower trace) trajectory. The parameters are  $N = 10$ ,  $\chi/J = 100$ ,  $f = 0.5$ , and  $\Gamma = 0.003$ .

tween the sides of that trap basically continuously. Evidently this works the better, the more numerous are the quantum jumps on the time scale of the variation of  $z(t)$ . For ten counts per one back-and-forth swing of the atoms,  $z_Q(t)$  for each single trajectory should give a good depiction of the experimental Josephson oscillations.

Classically, a trajectory exists objectively even without observations, but otherwise a similar correspondence between simulations and experiments prevails: If the classical description governed the experiments, each simulation according to Eqs. (9) and (10) would produce a representative outcome.

With this in mind, we present in Fig. 2 a classical (upper trace) and a quantum rendition (lower trace) of a single experiment for the same parameters as in Fig. 1(b). The collapse in Figs. 1 comes about from averaging over individual trajectories, and is absent here. In the mean-field theory and for each individual TWA trajectories, one expects strictly periodic oscillations in the classical trace. The deviations from periodicity in the classical trace originate from the phase diffusion. We have deliberately picked these random examples so that qualitatively similar classical and quantum behavior with occasional trapping of the populations in one or the other well is seen.

In our final Fig. 3 we go to such a small number of atom  $N = 10$  that one might seriously question the classical description, again with  $\chi/J = 10$ ,  $f = 0.5$ , and  $N_S = 1,000$ . In panel (a) we show the population imbalances as a function of time for both the quantum theory (solid line) and the classical theory (dashed line) without continuous monitoring,  $\Gamma = 0$ . Except for the initial collapse, there is little in common with the two traces, and one would conclude that the classical description is totally off at longer times. The proximate reason is that with a decreasing atom number  $N$  the quantum revivals start overlapping and produce an irregular-looking behavior that is absent in the classical approach. In panel (b) we have continuous measurements with  $\Gamma/J = 0.3$ , which again gives about ten photon counts during a back-and forth oscillation of the atoms. This time around the quantum and classical results qualitatively agree. It should be noted that the classical predictions for  $\Gamma/J = 0$

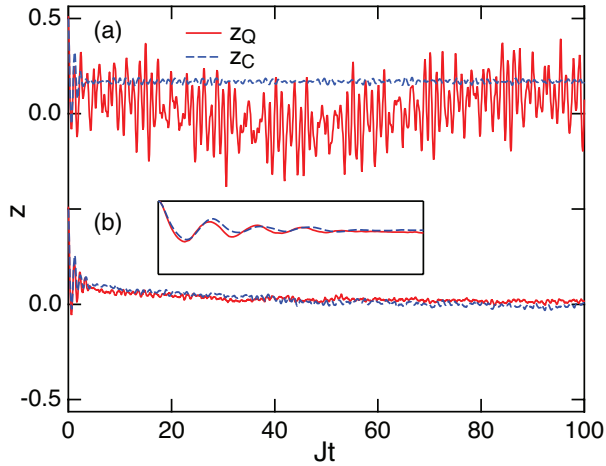


FIG. 3. (Color online) Quantum (solid lines) and classical (dashed lines) expectation values of population imbalance  $z$  as a function of time  $t$ . Graph (a) is without continuous monitoring,  $\Gamma/J = 0$ , for graph (b) the observation strength is  $\Gamma/J = 0.3$ . The atom number is  $N = 10$ , the rest of the parameters are as in Fig. 1. The inset expands the initial part of trace (b).

and  $\Gamma/J = 0.3$  are markedly different at long times, the latter seemingly tending toward  $z = 0$ . This tells us that the TWA ( $\Gamma/J = 0$ ) alone would not have worked in the case of Fig. 3(b). Here, to reach an agreement between the quantum and classical descriptions even in a trajectory-averaged quantity, it is necessary to include measurement back-action into both of them.

We have compared the exact quantum mechanical solution and a classical description of a BEC in a double-well

potential when the atom numbers in both sides of the trap are continuously monitored by light scattering. In the classical case we have amended the usual mean-field description in two ways. First, we have accounted for the quantum fluctuations in the initial state as in the TWA. Second, we have derived ab initio a diffusion for the relative phase of the BECs to account for the back-action of the measurements. The derivation was done specifically for the present example system, but the similar time reversal properties of Lindblad-form relaxation terms and of diffusion suggest that we have here a generic feature of physics.

The conjecture emerges is that if the measurements can resolve the classical behavior, that is what they do; quantum mechanics and a carefully crafted classical analysis are at least qualitatively equivalent. But, since we are encroaching into the regime where quantum mechanics is expected to have primacy, we might just as well say that a classical system behaves quantum mechanically. It is as if during continuous monitoring “classicality” leaks in from the measurement apparatus and blurs the border between quantum mechanics and classical mechanics.

Ultimately, we have introduced a scheme in a continuously monitored system that handles both quantum fluctuations and measurement back-action classically. Now, the computational resources required to solve the time evolution from quantum mechanics tend to increase very fast with the system size. We therefore hope to inspire practical methods to analyze time evolution when quantum effects are small but not negligible.

This work is supported in part by NSF, Grant No. PHY-0967644, the Leverhulme Trust, and the EPSRC.

- 
- [1] F. S. Cataliotti, S. Burger, C. Fort, P. Maddaloni, F. Minardi, A. Trombettoni, A. Smerzi, and M. Inguscio, *Science* **293**, 843 (2001).
  - [2] M. Albiez, R. Gati, J. Fölling, S. Hunsmann, M. Cristiani, and M. K. Oberthaler, *Phys. Rev. Lett.* **95**, 010402 (2005).
  - [3] S. Levy, E. Lahoud, I. Shomroni, and J. Steinhauer, *Nature* **449**, 579 (2007).
  - [4] T. Zibold, E. Nicklas, C. Gross, and M. K. Oberthaler, *Phys. Rev. Lett.* **105**, 204101 (2010).
  - [5] S. Raghavan, A. Smerzi, S. Fantoni, and S. R. Shenoy, *Phys. Rev. A* **59**, 620 (Jan 1999).
  - [6] J. Javanainen, *Phys. Rev. A* **81**, 051602 (2010).
  - [7] T. Spiller and J. Ralph, *Phys. Lett. A* **194**, A235 (1994).
  - [8] T. Brun, N. Gisin, P. O’Mahony, and M. Rigo, *Phys. Lett. A* **229**, A267 (1997).
  - [9] T. Bhattacharya, S. Habib, and K. Jacobs, *Phys. Rev. Lett.* **85**, 4852 (2000).
  - [10] S. Chaudhury, A. Smith, B. E. Anderson, S. Ghose, and P. S. Jessen, *Nature* **461**, 768 (2009).
  - [11] By classical description we mean one that obeys classical logic. This includes the usual probabilistic analysis.
  - [12] L. Isella and J. Ruostekoski, *Phys. Rev. A* **74**, 063625 (2006).
  - [13] P. B. Blakie, A. S. Bradley, M. J. Davis, R. J. Ballagh, and C. W. Gardiner, *Adv. Phys.* **57**, 363 (2008).
  - [14] A. Polkovnikov, *Ann. Phys. (N.Y.)* **325**, 1790 (2010).
  - [15] A. D. Martin and J. Ruostekoski, *Phys. Rev. Lett.* **104**, 194102 (2010).
  - [16] G. J. Milburn, J. Corney, E. M. Wright, and D. F. Walls, *Phys. Rev. A* **55**, 4318 (1997).
  - [17] J. Javanainen and M. Y. Ivanov, *Phys. Rev. A* **60**, 2351 (1999).
  - [18] C. Gardiner and P. Zoller, *Quantum Noise*, 3rd ed. (Springer, Berlin, 2004).
  - [19] J. Ruostekoski and D. F. Walls, *Phys. Rev. A* **58**, R50 (1998).
  - [20] J. Javanainen, unpublished (2011).
  - [21] D. F. Walls and G. J. Milburn, *Quantum Optics*, 2nd ed. (Springer, Berlin, 1994).
  - [22] J. Dalibard, Y. Castin, and K. Mølmer, *Phys. Rev. Lett.* **68**, 580 (1992).
  - [23] R. Dum, P. Zoller, and H. Ritsch, *Phys. Rev. A* **45**, 4879 (1992).
  - [24] L. Tian and H. J. Carmichael, *Phys. Rev. A* **46**, R6801 (1992).
  - [25] C. Gardiner, *Stochastic Methods*, 4th ed. (Springer, Berlin, 2009).